# Limits on the stochastic gravitational wave background and prospects for single-source detection with GRACE Follow-On

M. P. Ross,* C. A. Hagedorn, E. A. Shaw, A. L. Lockwood, B. M. Iritani, J. G. Lee, K. Venkateswara, and J. H. Gundlach

*Center for Experimental Nuclear Physics and Astrophysics, University of Washington, Seattle, Washington 98195, USA*

(Received 26 November 2019; accepted 6 May 2020; published 21 May 2020)

With a reinterpretation of recent results, the GRACE Follow-On mission can be applied to gravitational wave astronomy. Existing GRACE Follow-On data constrain the stochastic gravitational wave background to $\Omega_{\mathrm{GW}} < 3.3 \times 10^{7}$ at 100 mHz. With a dedicated analysis, GRACE Follow-On may be able to detect the inspiral of local neutron star binaries, inspiral of subgalactic stellar-mass black hole binaries, or mergers of intermediate-mass black hole binaries within the Milky Way.

DOI: 10.1103/PhysRevD.101.102004

## I. INTRODUCTION

GRACE Follow-On (GRACE-FO) [1] is a satellite mission currently in Earth orbit studying the terrestrial gravitational field. We show that by interpreting recent results from this mission as strain, one can (1) constrain the gravitational wave background and (2) provide an opportunity for single-source gravitational wave (GW) searches.

Incoherent GW must be present throughout the universe at some amplitude. A broadband stochastic background is one of the few observable consequences of cosmic inflation [2] and a signature of proposed exotic phenomena such as cosmic strings [3]. Measurements of, and constraints on, such a background would yield insight into of a wide range of phenomena, from inflationary models and predictions of string theory to populations of black holes and neutron stars. Existing limits on the stochastic background come from pulsar timing [4], satellite ranging [5,6], torsion balances [7,8], terrestrial interferometers [9], and geophysical observations [10–12].

The most prominent single-source GW are emitted either by binary systems or spinning asymmetric stars. While asymmetric stars emit GW with a quasi-stationary frequency, inspiraling binary systems radiate semimonotone GW before a rapid merger and ring-down phase. The only direct observations of GW have been from the merger of black hole binaries and binary neutron stars [13–15] by the LIGO [16] and Virgo [17] observatories.

## II. STRAIN MEASUREMENTS

As a GW passes two inertial masses nominally separated by a distance $x_0$ their relative displacement, $x$, is [18]:

$$x(t) = x_0 h_{xx} \cos(2\pi f t + \psi) \tag{1}$$

$$h_{xx} = h_{+}(\cos^2\theta\cos^2\phi - \sin^2\phi) + 2h_{\times}\cos\theta\sin\phi\cos\phi \tag{2}$$

where $h_{+,\times}$ are the plus and cross-polarization components of the gravitational wave, $\theta$ and $\phi$ are the polar and azimuthal angles of the source, $f$ is the wave frequency, and $\psi$ is an arbitrary phase. Here, the plus and cross polarizations are defined in the source frame.

The GRACE-FO satellite mission has produced sensitive relative-displacement measurements of an inertial mass pair formed by its two satellites separated by $x_0 = 220$ km. The published displacement spectrum [1] can be converted to strain via $\tilde{h}_{xx}(f) = \tilde{x}(f)/x_0$. The inferred strain-noise spectral density is shown in Fig. 1. As noted in Ref. [1],

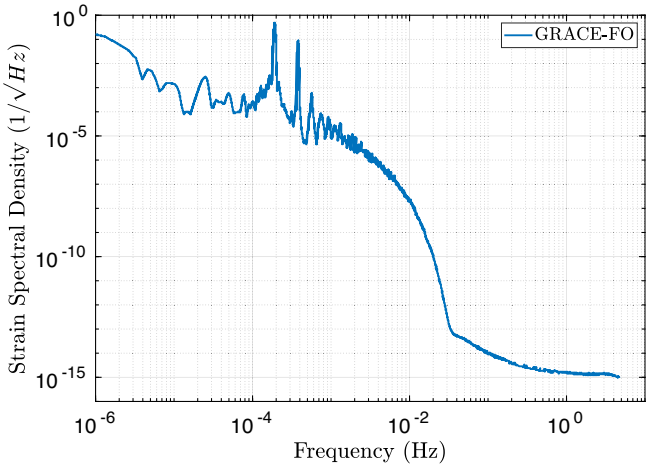


FIG. 1. Strain amplitude spectral density for the GRACE-FO mission. The increase in apparent noise below 30 mHz is due to terrestrial gravitational signals and not instrumental noise.

*mpross2@uw.edu

 

the noise below 30 mHz may be significantly reduced by subtracting models of the terrestrial gravitational field.

## III. BACKGROUND CONSTRAINTS

Assuming an isotropic, unpolarized, stochastic gravitational wave background, this strain noise can be interpreted as limits on the cosmological energy density of gravitational waves, $\Omega_{\rm GW}$ [19], by integrating Eq. (2) over incidence angle and polarization.

$$\Omega_{\rm GW}(f) = \frac{f}{\rho_{\rm crit}}\frac{{\rm d}\rho_{\rm GW}}{{\rm d}f} = \frac{32\pi^3}{3H_0^2} f^3 \frac{15}{4}\tilde{h}_{\rm meas}(f)^2 \qquad (3)$$

where $\rho_{\rm crit}$ is the critical energy density of the universe, $\rho_{\rm GW}$ is the energy density of gravitational waves, $H_0$ is Hubble constant, and $h_{\rm meas}$ is the measured displacement interpreted as strain. A Hubble constant of $H_0 = 70.3\ {\rm km\,s^{-1}\,Mpc^{-1}}$ was used [20]. The factor of $15/4$ corrects for the polarization and angular sensitivity of the instruments in question, see the Appendix A.

Confidence intervals were extracted from the GRACE-FO strain spectrum by separating the data into frequency bins which each encompassed 20 data points. Limits for each bin were set at the 95th percentile to yield the results shown in Fig. 2. We anticipate that a dedicated analysis would improve these constraints further.

## IV. SINGLE-SOURCES

In addition to setting stochastic GW limits, the GRACE-FO mission may allow for gravitational wave searches at frequencies between 30 mHz and 5 Hz. Both stellar-mass black hole binaries and neutron star binaries emit GW in the band of interest during their inspiral phase, while intermediate-mass black hole binaries would merge within the band.

Due to the orbit of the satellites, a GW seen by GRACE-FO would be modulated as the antenna pattern sweeps across the sky. This modulation can be approximated by rotating $\phi$ at the orbit frequency, $f_{\rm orb} = 1/94.5$ min [1].

$$\phi(t) = 2\pi f_{\rm orb} t + \phi_0 \qquad (4)$$

Simulated antenna factors [the angular dependence of Eq. (2)] for GRACE-FO, at a collection of $\theta$ values, are shown in Fig. 3. For sources in-line with the orbital axis ($\theta = 0$) the instrument's polarization sensitivity is modulated, while for sources in the orbital plane ($\theta = \pi/2$) the total observed power is modulated.

Detailed analysis of the orbit of the satellites and backgrounds due to the terrestrial gravitational field would be required for a definitive search. However, an estimate of the characteristic strain [21] sensitivity can be inferred from the strain spectral density. This is shown in Fig. 4 along with a collection of known and speculative sources. The best characteristic strain sensitivity is $2 \times 10^{-15}$ at 0.5 Hz.

The characteristic strain allows for the estimation of the signal-to-noise ratio (SNR) of an optimal search for a given source [21]. Figure 5 shows the estimated maximum detectable distance for a given equal component-mass system with a select SNR threshold.

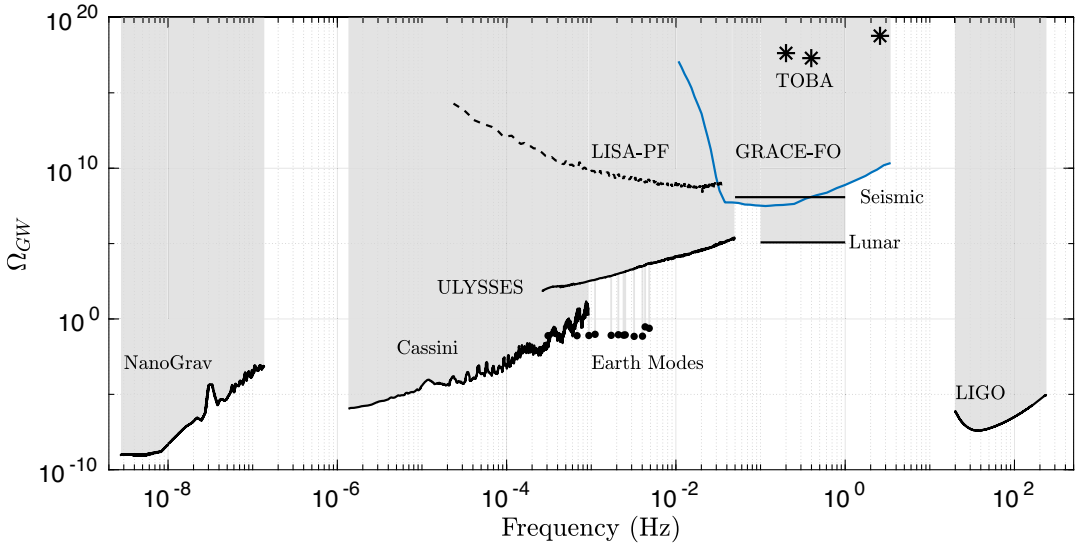


FIG. 2. Limits on the stochastic gravitational wave background set by GRACE-FO (blue) and LISA-PF (dashed). Analysis of LISA-PF is detailed in Appendix B. Additionally, limits set by NanoGrav [4], Cassini [5], ULYSSES [6], TOBA [7,8], LIGO [9], observations of the earth's normal modes [10], terrestrial seismic motion [11], and lunar seismic motion [12] are shown. Gray shading indicates regions excluded at 95% confidence.

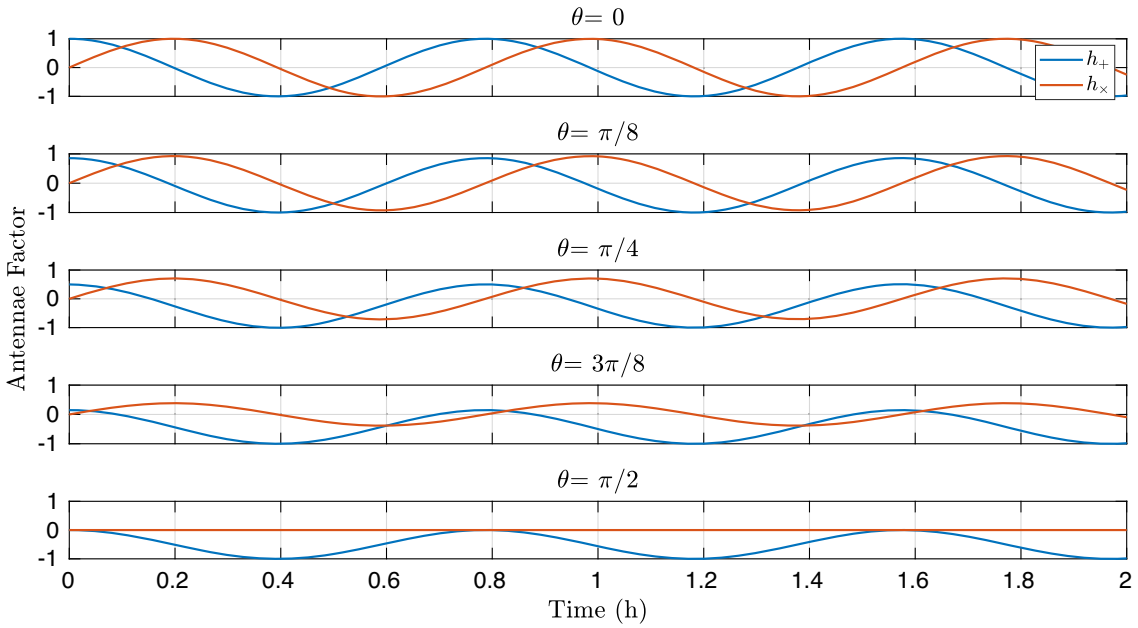


FIG. 3. Simulated antenna factors for $h_+$ and $h_\times$ where $\theta$ is the polar angle of the source. For sources in-line with the satellite's orbital axis ($\theta = 0$) the instrument's polarization sensitivity is modulated by the orbit, while for sources in the orbital plane ($\theta = \pi/2$) the total observed power is modulated.

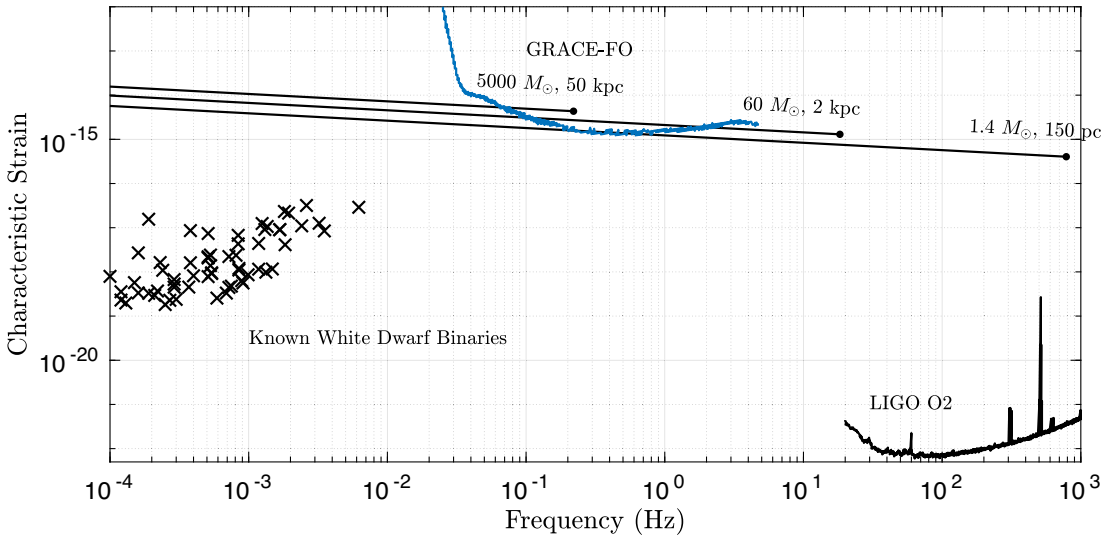


FIG. 4. Estimates of the characteristic strain sensitivity of GRACE-FO along with the expected strain from known white dwarf binaries [22–25] and a sensitivity curve for LIGO's second observing run [26]. Also shown are lines that correspond to the predicted characteristic strain of an equal component-mass 1.4 $M_\odot$ binary at 150 pc, a 60 $M_\odot$ at 2 kpc, and a 5000 $M_\odot$ at 50 kpc [21]. The points at the end of each line note the merger frequency for the corresponding system. These approximations are only valid for the inspiral phase of binary evolution.

The detection range peaks at component-masses of 2000–10000 $M_\odot$ with a volume encompassing most of the Milky Way. Above 10000 $M_\odot$, terrestrial gravitational signals severely limit detection capability while below ~100 $M_\odot$ the decreased emission does not provide an appreciable detection volume.

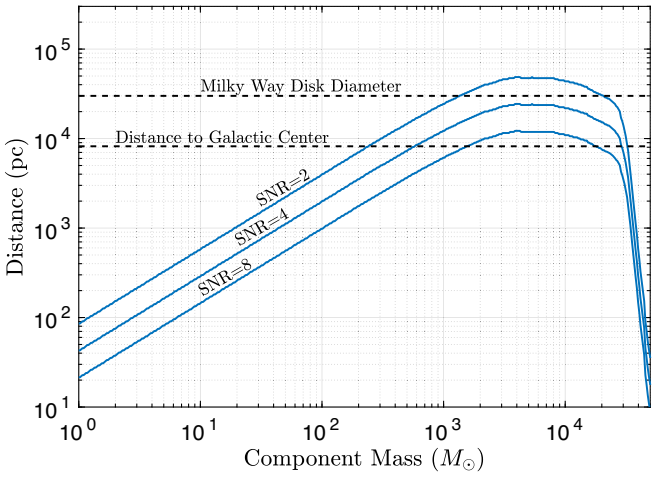


FIG. 5. Maximum detectable distance for equal component-mass binaries with SNR thresholds of 2, 4, and 8. For systems with component-mass of 2000–10000 $M_\odot$ the detection volume encompasses most of the Milky Way.

## V. CONCLUSION

Existing GRACE Follow-On data constrain the stochastic gravitational wave background to levels of $\Omega_{\mathrm{GW}} < 3.3 \times 10^7$ at 100 mHz. These constraints are many orders of magnitude from expected sources [2], yet provide an independent set of limits in a frequency range where existing limits are sparse.

With a dedicated analysis, GRACE-FO is capable of single-source GW searches. Promising target systems include the inspiral of local neutron star binaries or subgalactic stellar-mass black hole binaries, and the mergers of intermediate-mass black hole binaries within the Milky Way.

Although the application of this mission to gravitational wave astronomy will be supplanted by the launch of LISA [27], GRACE-FO has the capability to yield opportunistic insight into the local universe.

## ACKNOWLEDGMENTS

The authors would like to thank Eric Adelberger for his invaluable input and the anonymous referees for their insightful suggestions. This work was supported by funding from the NSF under Grants No. PHY-1607385, No. PHY-1607391, No. PHY-1912380 and No. PHY-1912514.

## APPENDIX A: INSTRUMENT RESPONSE

The strain along a single axis caused by a GW is [18]:

$$h_{xx} = h_+(\cos^2\theta\cos^2\phi - \sin^2\phi) + 2h_\times\cos\theta\sin\phi\cos\phi \tag{A1}$$

where $h_{xx}$ is the strain along the x-axis, $h_{+,\times}$ are the strain amplitudes respectively in the plus and cross polarization, and $\theta$ and $\phi$ are the polar and azimuth angles, respectively.

Assuming isotropic emission, the fraction of incident power that is captured by a single-axis instrument can be found by:

$$\tilde{h}^2_{\mathrm{meas}}(f) = \frac{1}{4\pi}\int \tilde{h}^2_{xx}(f)d\Omega$$

$$= \frac{1}{4\pi}\int d\Omega[\tilde{h}^2_+(f)(\cos^2\theta\cos^2\phi - \sin^2\phi)^2 \tag{A2}$$

$$+ 4\tilde{h}^2_\times(f)(\cos\theta\sin\phi\cos\phi)^2$$

$$+ 2\tilde{h}_+(f)\tilde{h}_\times(f)(\cos^2\theta\cos^2\phi - \sin^2\phi)$$

$$\times\cos\theta\sin\phi\cos\phi] \tag{A3}$$

$$= \frac{1}{4\pi}\left(\tilde{h}^2_+(f)\frac{22\pi}{15} + 4\tilde{h}^2_\times(f)\frac{\pi}{6}\right). \tag{A4}$$

Further assuming an unpolarized background, the polarization can be averaged to yield:

$$\tilde{h}^2_+(f) = \tilde{h}^2_\times(f) = \frac{1}{2}\tilde{h}^2(f) \tag{A5}$$

$$\tilde{h}^2_{\mathrm{meas}}(f) = \frac{1}{8\pi}\tilde{h}^2(f)\left(\frac{22\pi}{15} + \frac{2\pi}{3}\right) \tag{A6}$$

$$\tilde{h}^2_{\mathrm{meas}}(f) = \frac{4}{15}\tilde{h}^2(f). \tag{A7}$$

## APPENDIX B: LISA PATHFINDER

The technique used with GRACE-FO can also be applied to LISA Pathfinder (LISA-PF) [28] which was flown to demonstrate the drag-free technology needed for the future

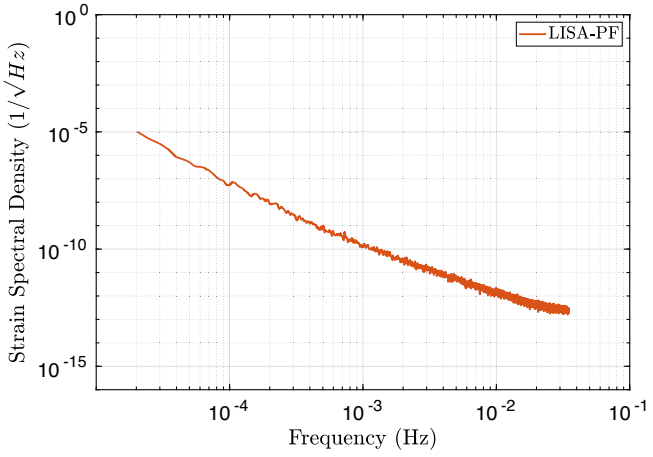


FIG. 6. Strain amplitude spectral density for LISA-PF.

LISA mission [27]. For LISA-PF the mass-pair is formed by the proof masses, separated by $x_0 = 376$ mm. LISA-PF has published an acceleration noise spectrum which can be converted to strain via $\tilde{h}_{xx}(f) = -\frac{1}{x_0\omega^2}\tilde{\ddot{x}}(f)$. The corresponding strain spectral density is shown in Fig. 6. This measurement can constrain the stochastic gravitational wave background to $\Omega_{\rm GW} < 6.5 \times 10^8$ at 10 mHz as seen in Fig. 2.


[1] K. Abich *et al.*, In-Orbit Performance of the GRACE Follow-On Laser Ranging Interferometer, Phys. Rev. Lett. **123**, 031101 (2019).

[2] R. Easther and E. A. Lim, Stochastic gravitational wave production after inflation, J. Cosmol. Astropart. Phys. 04 (2006) 010.

[3] T. Damour and A. Vilenkin, Gravitational radiation from cosmic (super)strings: Bursts, stochastic background, and observational windows, Phys. Rev. D **71**, 063510 (2005).

[4] Z. Arzoumanian *et al.*, The NANOGrav 11-year data set: High-precision timing of 45 millisecond pulsars, Astrophys. J. Suppl. Ser. **235**, 37 (2018).

[5] J. W. Armstrong, L. Iess, P. Tortora, and B. Bertotti, Stochastic gravitational wave background: Upper limits in the $10^{-6}$ to $10^{-3}$ Hz band, Astrophys. J. **599**, 806 (2003).

[6] B. Bertotti, R. Ambrosini, J. W. Armstrong, S. W. Asmar, G. Comoretto, G. Giampieri, L. Iess, Y. Koyama, A. Messeri, A. Vecchio, and H. D. Wahlquist, Search for gravitational wave trains with the spacecraft ULYSSES, Astron. Astrophys. **296**, 13 (1995).

[7] K. Ishidoshiro, M. Ando, A. Takamori, H. Takahashi, K. Okada, N. Matsumoto, W. Kokuyama, N. Kanda, Y. Aso, and K. Tsubono, Upper Limit on Gravitational Wave Backgrounds at 0.2 Hz with a Torsion-Bar Antenna, Phys. Rev. Lett. **106**, 161101 (2011).

[8] A. Shoda, Y. Kuwahara, M. Ando, K. Eda, K. Tejima, Y. Aso, and Y. Itoh, Ground-based low-frequency gravitational-wave detector with multiple outputs, Phys. Rev. D **95**, 082004 (2017).

[9] B. P. Abbott *et al.*, Search for the isotropic stochastic background using data from Advanced LIGO's second observing run, Phys. Rev. D **100**, 061101 (2019).

[10] M. Coughlin and J. Harms, Constraining the gravitational wave energy density of the universe using earth's ring, Phys. Rev. D **90**, 042005 (2014).

[11] M. Coughlin and J. Harms, Upper Limit on a Stochastic Background of Gravitational Waves from Seismic Measurements in the Range 0.05–1 hz, Phys. Rev. Lett. **112**, 101102 (2014).

[12] M. Coughlin and J. Harms, Constraining the gravitational-wave energy density of the universe in the range 0.1 Hz to 1 Hz using the Apollo Seismic Array, Phys. Rev. D **90**, 102001 (2014).

[13] B. P. Abbott *et al.*, GWTC-1: A Gravitational-Wave Transient Catalog of Compact Binary Mergers Observed by LIGO and Virgo during the First and Second Observing Runs, Phys. Rev. X **9**, 031040 (2019).

[14] B. P. Abbott *et al.*, GW190425: Observation of a compact binary coalescence with total mass $\sim 3.4\ M_\odot$, Astrophys. J. Lett. **892**, L3 (2020).

[15] LIGO Scientific and Virgo Collaboration, GW190412: Observation of a binary-black-hole coalescence with asymmetric masses, arXiv:2004.08342.

[16] J. Aasi *et al.*, Advanced LIGO, Classical Quantum Gravity **32**, 074001 (2015).

[17] F. Acernese *et al.*, Advanced Virgo: A second-generation interferometric gravitational wave detector, Classical Quantum Gravity **32**, 024001 (2015).

[18] M. Maggiore, *Gravitational Waves: Volume 1: Theory and Experiments* (Oxford University Press, Oxford, 2008), Vol. 1.

[19] B. Allen and J. D. Romano, Detecting a stochastic background of gravitational radiation: Signal processing strategies and sensitivities, Phys. Rev. D **59**, 102001 (1999).

[20] K. Hotokezaka, E. Nakar, O. Gottlieb, S. Nissanke, K. Masuda, G. Hallinan, K. P. Mooley, and A. T. Deller, A Hubble constant measurement from superluminal motion of the jet in GW170817, Nat. Astron. **3**, 940 (2019).

[21] C. J Moore, R. H Cole, and C. P L Berry, Gravitational-wave sensitivity curves, Classical Quantum Gravity **32**, 015014 (2015).

[22] V. Korol, E. M. Rossi, P. J. Groot, G. Nelemans, S. Toonen, and A. G. A. Brown, Prospects for detection of detached double white dwarf binaries with Gaia, LSST and LISA, Mon. Not. R. Astron. Soc. **470**, 1894 (2017).

[23] K. B. Burdge, J. Fuller, E. S. Phinney, J. van Roestel, A. Claret, E. Cukanovaite, N. P. G. Fusillo, M. W. Coughlin, D. L. Kaplan, T. Kupfer, P.-E. Tremblay, R. G. Dekany, D. A. Duev, M. Feeney, R. Riddle, S. R. Kulkarni, and T. A. Prince, Orbital decay in a 20 minute orbital period detached binary with a hydrogen-poor low-mass white dwarf, Astrophys. J. **886**, L12 (2019).

[24] J. J. Hermes, M. Kilic, W. R. Brown, D. E. Winget, C. A. Prieto, A. Gianninas, A. S. Mukadam, A. Cabrera-Lavers, and S. J. Kenyon, Rapid orbital decay in the 12.75-minute binary white dwarf $J0651 + 2844$, Astrophys. J. **757**, L21 (2012).

[25] K. B. Burdge, M. W. Coughlin, J. Fuller, T. Kupfer, E. C. Bellm, L. Bildsten, M. J. Graham, D. L. Kaplan, J. Van

Roestel, R. G. Dekany *et al.*, General relativistic orbital decay in a seven-minute-orbital-period eclipsing binary system, Nature (London) **571**, 528 (2019).

[26] J. C. Driggers *et al.*, Improving astrophysical parameter estimation via offline noise subtraction for Advanced LIGO, Phys. Rev. D **99**, 042001 (2019).

[27] K. Danzmann (LISA Study Team), LISA: Laser interferometer space antenna for gravitational wave measurements, Classical Quantum Gravity **13**, A247 (1996).

[28] M. Armano *et al.*, Beyond the Required LISA Free-Fall Performance: New LISA Pathfinder Results Down to 20 $\mu$Hz, Phys. Rev. Lett. **120**, 061101 (2018).